

Automated Retinal Vessel Segmentation using Entropic Thresholding Based Spatial Correlation Histogram of Gray Level Images

Soumia Belhadi and Nadjia Benblidia
Faculty of science, Saad Dahlab University, Algeria

Abstract: After highlighting vessel like structure by an appropriate filter in Matched Filter (MF) technique, thresholding strategy is needed for the automated detection of blood vessels in retinal images. For the purpose, we propose to use a new technique of entropic thresholding based on Gray Level Spatial Correlation (GLSC) histogram which takes into account the image local property. Results obtained show robustness and high accuracy detection of retinal vessel tree. An appropriate technique of thresholding allows significant improvement of the retinal vessel detection method.

Keywords: Automated screening, retinal vessel segmentation, matched filtering, thresholding.

Received July 20, 2012; accepted January 29, 2013; published online September 4, 2014

1. Introduction

Diabetic retinopathy is a severe complication of diabetes. It damages blood vessels inside the retina causing vision loss and blindness [3]. It is important to screen patients with diabetes regularly for the development of retinal disease [10] because the vast majority of patients who develop diabetic retinopathy have no symptoms until the very late stages. A computerized screening system can be used for fully automated mass screening. Such systems screen a large number of retinal images and identify abnormal images. This would save a significant amount of workload and time for ophthalmologists. The identification of the blood vessels constitutes an important step in the design of systems for automated screening and analysis of diabetic retinopathy. Many methods for retinal vessel segmentation have been reported. After studying a vast majority of the literature, we can divide these methods into five main categories: Category of supervised approaches [5], category of tracking approaches, category of skeleton based and ridge based approaches, category of model based approaches [2, 4, 12, 16] and finally the category of approaches which adopts the principle of bringing out the vascular structure by an appropriate filters and then generating a binary image by thresholding or by pixel classification. It regroups the set of the following methods: Wavelet based methods; mathematical morphology based methods and Matched Filter (MF) methods [14, 18].

MF techniques convolve the image with multiple MFs in different orientations and sizes [17]. Considering the fact that the cross-section of a vessel can be modeled as a gaussian function [1], a series of gaussian shaped filters can be used. MF technique allows the enhancement and the detection of vessels in

real time. The filters used are sensitive to vessels of different orientation, thickness and contrast.

MF method doesn't work alone; it should be part of a whole algorithmic chain. It provides a non-binary image that still needs classification into background or vessel. Threshold is used to divide the range of intensity of the MF response image into two classes which are applied locally or globally. Chaudhuri [1] an automatic thresholding algorithm that maximizes the inter-class intensity variance was used to binarize the enhanced image. Zhang *et al.* [20] the vessels are detected by thresholding the MF response image while the threshold is adjusted by the images response to the first derivative of gaussian. Hoover *et al.* [7] proposed an iterative process, called threshold probing, in which the threshold value used in a region growing process is optimized, based on tests realized on the detected vessel region. Sometimes, several enhanced images are combined, using probabilistic approach [9] or a fuzzy formalism [13] to achieve the fusion.

In the present work, we propose to use for the first time a new technique of thresholding, based on information theory [19], for the classification of the MF pixels response into vessels and background in retinal images. The technique proposed by Xiao *et al.* [19], called: "entropic thresholding based on gray level special correlation histogram", achieves better performance than 1D methods with less time consumption. The method takes into account the image local property by the Gray Level Spatial Correlation (GLSC) histogram defined by the authors. This technique was never used in the context of our study.

The rest of the paper is organized as follows: Next section explains and illustrates the proposed method of retinal vessels detection and gives detailed description about the entropic thresholding technique adopted. While section 3 describes the material used in this

study and presents the results obtained and compare them to those obtained with other existing methods. Finally, conclusions and discussion conclude this paper.

2. Our Proposed Method

For a robust and efficient detection of blood vessels, we describe in this section our new approach based on MFs technique and a special entropic thresholding. The method is carried out in the various stages. Figure 1 shows the block diagram of our proposed method.

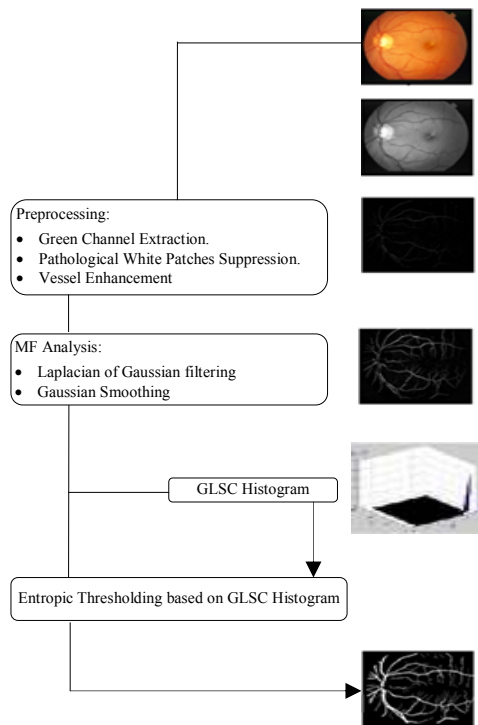


Figure 1. The different steps of our blood vessel segmentation method.

The following process stages may be identified: Original fundus image pre-processing for pathological white patches suppression and blood vessel enhancement., matched filtering for piecewise linear segments detection and entropic thresholding based on gray-level spatial correlation histogram for blood vessel tree extraction.

Input images are monochrome and obtained by extracting the green band from original RGB retinal images because the green channel provides the best vessel-background contrast of the RGB-representation [6].

2.1. Morphological Pre-Processing

Color fundus images often show important lighting variations, poor contrast and the presence of different lesions. In order to, reduce these degradations [8] a preprocessing for: Pathological white patches suppression and vessel enhancement is performed.

- **Pathological White Patches Suppression:** The aim of this section is the suppression of some bright lesions, known as cotton wool spots. Supremum of

openings using linear structuring element in different orientations is applied to the green plane of the image. The length of the structuring element is fixed to be able to contain a largest cotton wool spot possible

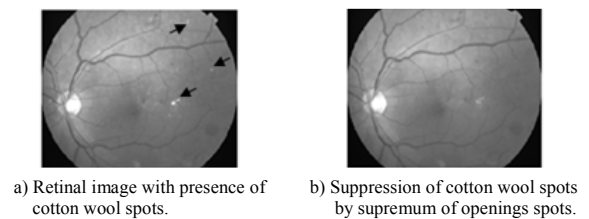


Figure 2. Pathological white patches suppression.

- **Vessel Enhancement:** The method for vessel enhancement uses top-hat transform as follows. Let g represent the green channel of the test image after pathological white patches suppression. Firstly, blood vessels are eliminated by a closing operation using a square structuring element s_1B of length s_1 larger than the maximal width of blood vessels d_{max} . A typical value of d_{max} is 7 pixels for an eye fundus image of 700 rows Figure 3-b.

$$h_1 = \varphi^{s_1 b}(g) \quad (1)$$

Secondly, image subtraction is performed as follow: Figure 3-c.

$$h_2 = h_1 - g \quad (2)$$

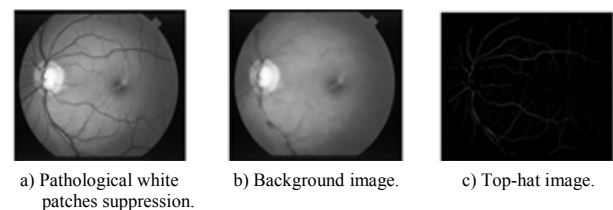


Figure 3. Illustration of the vessel enhancement process.

2.2. Matched Filtering

In the present work, to distinguish vessels from other non-tubular structures, we adopt a method based on the use of the laplacian of gaussian filter to highlight retinal vessels [15]. Figure 4 shows the effect of the second derivative of a gaussian signal.

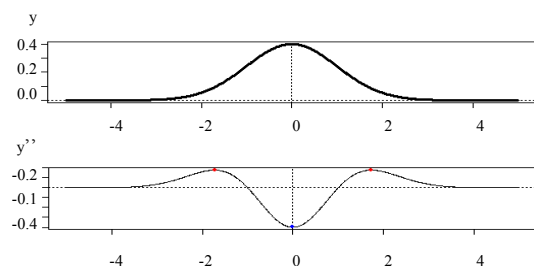


Figure 4. Second derivative of two dimensional gaussian signal.

In addition, the image is gaussian smoothed to counter the problem of the high sensitivity of the laplacian of gaussian filter to noise. Thus, two one dimensional kernels are applied successively. The

kernel in the tangential direction is simply a gaussian function G_θ and the kernel in the normal direction is the second order derivative of the gaussian function G_θ . Twelve templates at different orientations are used to fit into vessels of different configuration. The negative values of the results are then set to zero and the maximum response is taken. The MF response is calculated as follows:

$$M = \sup_{\theta} (-h_2 * G_\theta * G_{\theta=90}) \quad (3)$$

Where

- $G_\theta(r)$: One dimensional gaussian filter in polar coordinates.

$$G_\theta(r) = \frac{1}{\sqrt{2\pi\sigma^2}} \exp\left(-\frac{r^2}{2\sigma^2}\right) \quad (4)$$

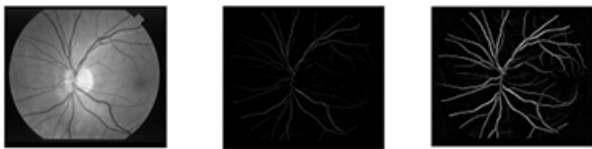
- $G''_\theta(r)$: One dimensional laplacian of gaussian filter in polar coordinates.

$$G''_\theta(r) = \frac{k(r^2 - \sigma^2)}{\sigma^4} \exp\left(-\frac{r^2}{2\sigma^2}\right) \quad (5)$$

And

- (θ, r) : Polar coordinates. θ varies between 0 and 165 degrees with step of 15 degrees.
- K : The weighting coefficient. In our case, we choose $K=1$.
- σ : Standard deviation of the gaussian kernel. According to chaudhuri and al model [1], $\sigma=2$ for kernel of dimension 9×9 .

Figure 5 Shows an example of retinal image after pre-processing stage and its MF response with a very significant enhancement of blood vessels.



a) Original retinal image. b) Pre-processed retinal image. c) MF response.

Figure 5. MF process.

2.3. Entropic Thresholding

The MFR image is processed by a proper thresholding scheme. In order to, extract the vessel segments from the background. An efficient entropy-based thresholding algorithm, which takes into account the spatial distribution of gray levels, is used. Specifically, we implement a local entropy thresholding technique, described in [19] which can apply the image local property to thresholding and reduce the time consumption. The proposed entropic thresholding method is based on the GLSC histogram defined by the authors. The GLSC histogram takes into account the image local property by using the gray value of the pixels and their similarity with neighboring pixels in gray value. It is calculated as follows: Let $M(x, y)$ be the gray value of the pixel located at the position (x, y) in a MF response image of size $H \times W$. We denote the set of all gray levels $\{0, 1, 2, \dots, 255\}$ as G . We

defined a descriptor function $g(x, y)$ for each pixel $M(x, y)$ as a number of pixels for which the gray value is close to it (measure of similarity using parameter ξ) in the corresponding $N \times N$ neighborhood, where N is a positive number. $g(x, y)$ is calculated as follows:

$$g(x, y) = \sum_{i=-\frac{N-1}{2}}^{\frac{N-1}{2}} \sum_{j=-\frac{N-1}{2}}^{\frac{N-1}{2}} \text{fct}\left(\left[|M(x+i, y+j) - M(x, y)|\right], \xi\right) \quad (6)$$

Where

$$\text{fct}\left(\left[|M(x+i, y+j) - M(x, y)|\right], \xi\right) = \begin{cases} 1 & \text{if } |M(x+i, y+j) - M(x, y)| \leq \xi \\ 0 & \text{if } |M(x+i, y+j) - M(x, y)| > \xi \end{cases} \quad (7)$$

The choice of parameters ξ and N is discussed in section 3.

The GLSC histogram value $h(k, m)$ represents the rate of pixels in the image having a gray value k and m similar pixels in a window of size $N \times N$. The value of $h(k, m)$ at each position (k, m) : $k \in G$ and $m \in \{1, 2, \dots, N \times N\}$ is calculated as follows:

$$h(k, m) = \text{prob}(M(x, y) = k \text{ and } g(x, y) = m) \quad (8)$$

The next formula allows the approximation of the normalized GLSC histogram:

$$\hat{h}(k, m) = \frac{\text{number of pixels with gray value } k \text{ and } m \text{ pixels of similar gray value in } N \times N \text{ neighborhood}}{\text{number of pixels in the whole image}} \quad (9)$$

Figure 6 shows retinal fundus image, its original gray-level histogram and GLSC histogram corresponding to $N=3$ and $\xi=4$. Objects and background are usually the major part in the image and their gray value is relatively homogeneous compared with noise and edge. Consequently, the regions with high m value in GLSC histogram correspond to objects or background more probably while the regions with low m value correspond to noise or edge oppositely.



a) MF response of retinal image.

b) Its gray level histogram.

c) Its GLSC histogram.

Figure 6. GLSC histogram.

Thresholding stage aims at finding an optimum threshold t which partitionates the set of gray levels G into two disjoint subsets $G_A = \{0, 1, \dots, t\}$ and $G_B = \{t+1, \dots, 255\}$, where G_A denotes the background and G_B the vascular structure. The probability distributions associated with background and vessels are given by:

$$\left[\frac{p(0, I)}{p_A(t)}, \dots, \frac{p(0, N * N)}{p_A(t)}, \frac{p(I, I)}{p_A(t)}, \dots, \frac{p(t, N * N)}{p_A(t)} \right] \quad (10)$$

And

$$\left[\frac{p(t+1, I)}{p_B(t)}, \dots, \frac{p(t+1, N * N)}{p_B(t)}, \frac{p(t+2, I)}{p_B(t)}, \dots, \frac{p(255, N * N)}{p_B(t)} \right] \quad (11)$$

Where

$$p(k, m) = \hat{h}(k, m) \tag{12}$$

$$p_A(t) = \sum_{k=0}^t \sum_{m=1}^{N^*N} p(k, m) \tag{13}$$

$$p_B(t) = \sum_{k=t+1}^{255} \sum_{m=1}^{N^*N} p(k, m) \text{ and } p_A(t) + p_B(t) = 1 \tag{14}$$

The threshold selection is based on the entropy theory. The class entropies are defined for the retinal vessels and the background. The maximization of the total entropy of the partitioned image, interpreted as a measure of separability, is then achieved.

Elements of the GLSC histogram should not be treated equally in entropy evaluation because edges constitute an important indicator of vessels and can yield more information about the textural contents of the retinal image. The entropy calculation of elements in GLSC histogram are weighted by a nonlinear function associated with m and N given by:

$$Weight(m, N) = \frac{1 + e^{-\frac{2m}{N^*N}}}{1 - e^{-\frac{2m}{N^*N}}} \tag{15}$$

The entropies associated with background and vessels are given by:

$$H_A(t, N) = - \sum_{k=0}^t \sum_{m=1}^{N^*N} \frac{p(k, m)}{p_A(t)} \ln \frac{p(k, m)}{p_A(t)} Weight(m, N) \tag{16}$$

$$H_B(t, N) = - \sum_{k=t+1}^{255} \sum_{m=1}^{N^*N} \frac{p(k, m)}{p_B(t)} \ln \frac{p(k, m)}{p_B(t)} Weight(m, N) \tag{17}$$

The following function is used as a criterion function:

$$\phi(t, N) = H_A(t, N) + H_B(t, N) \tag{18}$$

We obtain the optimal threshold t^* by maximizing

$$\phi(t, N); t^* = Arg \max \phi(t, N) \tag{19}$$

After entropic thresholding, a binary image is obtained representing retinal vessel tree.

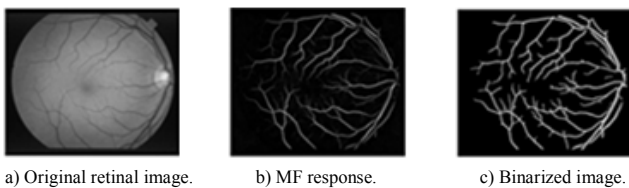


Figure 7. Examples of entropic thresholding.

3. Experimental Results and Discussion

3.1. Description of the Used Databases

To evaluate the vessel segmentation methodology described in section 2, a publicly available database containing retinal images, the Structured Analysis of Retina (STARE) [11] database, was used. This database has been widely used by other researchers to test their vessel segmentation methodologies it provides manual segmentations for performance evaluation. The STARE database, originally collected by Hoover and Goldbaum [6] contains twenty retinal

fundus slides and their ground truth images. All the twenty images were carefully labeled by hand to produce ground truth vessel segmentation by an expert.

3.2. Evaluation of Our Approach

Quantitative evaluation of the segmentation algorithm is done by comparing the output image with the corresponding manually segmented image of the STARE database. The comparison yields statistical measures that can be summarized using contingency table, as shown in Table 1.

Table 1. Contingency table.

		Ground Truth	
		Vessel Present	Vessel Absent
Method Result	Vessel Detected	True Positive (TP)	False Positive (FP)
	Vessel Not Detected	False Negative (FN)	True Negative (TN)

In this paper, our algorithm was evaluated in terms of Sensitivity (Se), Specificity (Sp) and Accuracy (Acc). Taking Table 1 into account, these metrics are defined as:

$$Se = \frac{TP}{TP + FN} \tag{20}$$

$$Sp = \frac{TN}{TN + FP} \tag{21}$$

$$Acc = \frac{TP + TN}{TP + FN + TN + FP} \tag{22}$$

Se gives the percentage of pixels correctly classified as vessels by the method and Sp gives the percentage of non-vessels pixels classified as non-vessels by the method. Finally, Acc is a global measure providing the ratio of total well-classified pixels.

From the results of Table 2, we conclude that when $\zeta=4$, the proposed thresholding method produced the best optimal threshold values.

For experiment, we ever consider neighborhood sizes of 3×3 , 5×5 , 7×7 , 9×9 and 11×11 to obtain $h(k, m)$ respectively. Increasing the number of neighborhood did not result in significant improvement of result but increased the time consumption.

Thresholding approach proposed in this paper provides the highest average when choosing neighborhood size of 3×3 with $\zeta=4$.

Table 2. Threshold and accuracy values for various values of ζ on STARE images.

Image	$\zeta=0$		$\zeta=1$		$\zeta=2$		$\zeta=3$		$\zeta=4$		$\zeta=5$	
	t*	Acc										
01	50	0.9378	47	0.9399	44	0.9487	42	0.9488	42	0.9488	42	0.9488
02	70	0.7500	43	0.9500	43	0.9500	43	0.9500	43	0.9500	43	0.9500
03	69	0.9710	110	0.8711	69	0.9710	69	0.9710	70	0.9714	70	0.9714
04	30	0.9512	30	0.9512	31	0.9514	31	0.9514	32	0.9516	32	0.9516
05	53	0.9555	53	0.9555	52	0.9557	52	0.9557	52	0.9557	52	0.9557
06	60	0.6985	44	0.8855	35	0.9655	35	0.9655	35	0.9655	35	0.9655
07	80	0.8559	46	0.9569	46	0.9569	46	0.9569	46	0.9569	46	0.9569
08	48	0.9008	48	0.9008	48	0.9008	48	0.9008	45	0.9558	45	0.9558
09	47	0.9627	48	0.9627	48	0.9627	48	0.9627	48	0.9627	48	0.9627
10	56	0.9614	60	0.9541	58	0.9611	58	0.9614	56	0.9614	56	0.9614
11	45	0.9651	45	0.9651	45	0.9651	42	0.9661	41	0.9666	41	0.9666
12	70	0.8699	55	0.9600	41	0.9722	41	0.9722	41	0.9722	41	0.9722
13	42	0.9612	42	0.9612	42	0.9612	42	0.9612	40	0.9620	40	0.9620
14	62	0.8336	57	0.8699	41	0.9623	41	0.9623	41	0.9623	41	0.9623
15	38	0.9590	38	0.9590	38	0.9590	39	0.9580	37	0.9591	37	0.9591
16	57	0.9045	50	0.9450	48	0.9452	48	0.9452	47	0.9453	47	0.9453
17	45	0.9570	43	0.9572	45	0.9570	45	0.9570	43	0.9572	43	0.9572
18	40	0.9772	31	0.9774	31	0.9774	31	0.9774	31	0.9774	31	0.9774
19	47	0.9757	47	0.9757	47	0.9757	30	0.9771	32	0.9777	32	0.9777
20	40	0.9559	42	0.9558	42	0.9558	39	0.9560	38	0.9561	38	0.9561

Figure 8 shows an example of results obtained with our method on retinal images available on STARE database and a comparison with ground truth. The results are listed in Table 3 and the last row of the table shows average Sp , Se and Acc for the 20 images of the database. The thresholding stage is performed with neighborhood size of 3×3 and $\zeta = 4$.

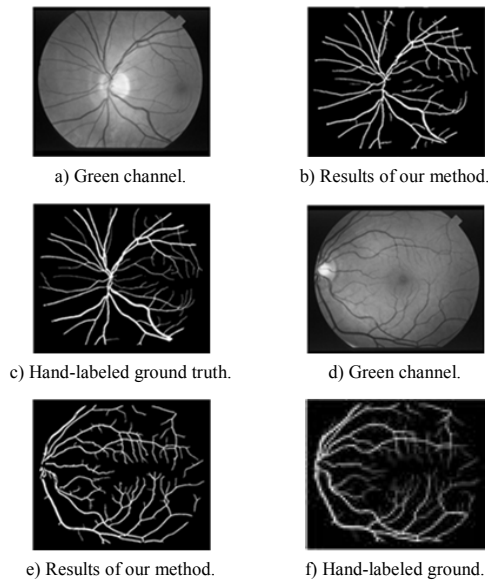


Figure 8. Blood vessel detection results.

Table 3. Performance results on STARE database images.

Image	Se	Sp	Acc
01	0.6448	0.9835	0.9488
02	0.6913	0.9821	0.9500
03	0.6204	0.9937	0.9714
04	0.5107	0.9949	0.9516
05	0.7273	0.9784	0.9557
06	0.7325	0.9829	0.9655
07	0.8615	0.9652	0.9569
08	0.8689	0.9628	0.9558
09	0.8102	0.9757	0.9627
10	0.7724	0.9779	0.9614
11	0.7888	0.9803	0.9666
12	0.8095	0.9858	0.9722
13	0.7005	0.9876	0.9620
14	0.7123	0.9872	0.9623
15	0.6246	0.9907	0.9591
16	0.5394	0.9915	0.9453
17	0.8778	0.9650	0.9572
18	0.7273	0.9960	0.9774
19	0.6506	0.9924	0.9777
20	0.4998	0.9946	0.9561
Average	0.7085	0.9834	0.9624

The results obtained show that our method is good for detecting large and small vessels concurrently, because the GLSC histogram takes into account the image local property by using the gray value of the pixels and their similarity with neighboring pixels in gray value, which is different from the other methods of thresholding. Thus, pixels representing very small and low contrasted vessels are taking into account in a thresholding stage thanks to the use of the weighted function described in section 2.

The results of the proposed method are also compared with those of Chaudhuri *et al.* [1, 7], on twenty images from the STARE database and the result is depicted in Table 4. The values shown in Table 4 about Hoover *et al.* [7] method and Niemeijer [11] method are presented for STARE database as reported

by their authors. In Figure 9, it can be clearly visualized that the proposed method reaches better performance than Hoover *et al.* method [7].

Table 4. Comparison of vessel segmentation results on STARE database with other methods.

Method	Acc (%)
Proposed Method	96
Hoover <i>et al.</i> [7]	92
Chaudhuri [1]	87

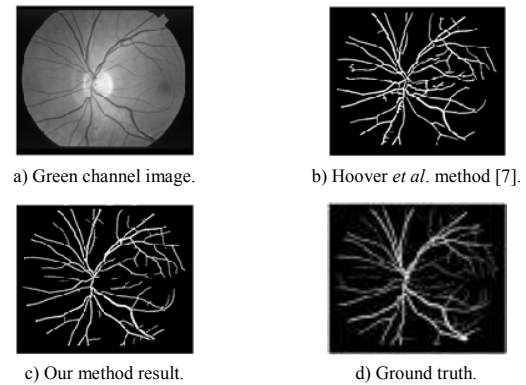


Figure 9. Results obtained with our method and a comparison with ground truth.

In addition, method simplicity should also be highlighted. The vessel segmentation algorithm is based on thresholding the MF response, thus needing shorter computational time. The entire process of segmenting vessels was performed on Intel PC with 2.53 GHz CPU and 4, 00 Go memory. The processing of each image including convolution and thresholding took about 10 seconds.

4. Conclusions

We have previously described a variety of techniques employed in retinal image processing for the identification of retinal blood vessels. This study has added to the previous work by showing that the thresholding technique is of a great prominence in the improvement of the detection method. We have used and adapted a new entropic thresholding technique based on GLSC histogram for the detection of retinal vessel tree by a MF approach.

Performance of the system has been evaluated on a STARE database. Results obtained show robustness and high Acc detection of retinal vessel tree thanks to entropic thresholding approach adopted which takes into account the image local property by using the gray value of the pixels and their similarity with neighboring pixels in gray value.

The demonstrated effectiveness and robustness, together with its simplicity and fast implementation, make this proposed automated blood vessel segmentation method a suitable tool for being integrated into a complete prescreening system for early diabetic retinopathy detection.

The performance of the proposed method can be improved by involving in the pre-processing scheme,

the anatomical constraints of vessels to enhance only vascular structures for further processing and thus increasing the specificity rate.

References

- [1] Chaudhuri S., "Detection of Blood Vessels in Retinal Images using Two-Dimensional Matched filters," *IEEE Transaction on Medical Imaging*, vol. 8, no. 3, pp. 263-269, 1989.
- [2] Cree M., Cornforth D., and Jelinek H., "Vessel Segmentation and Tracking using a Two-Dimensional Model," in *Proceedings of Image and Vision Computing Conference*, Dunedin, New Zealand, pp. 345-350, 2005.
- [3] Dodson P., "Diabetic Retinopathy: Treatment and Prevention," *Diabetes and Vascular Disease Research*, vol. 4, no. 3, pp. 9-11, 2007.
- [4] Espona L., Carreira M., Penedo M., and Ortega M., "Retinal Vessel Tree Segmentation using a Deformable Contour Model," in *Proceedings of the 19th International Conference on Pattern Recognition*, Florida, USA, pp. 1-4, 2008.
- [5] Gardner G., Keating D., Williamson T., and Elliott A., "Automatic Detection of Diabetic Retinopathy using an Artificial Neural Network: A Screening Tool," *British Journal of Ophthalmology*, vol. 80, no. 11, pp. 940-944, 1996.
- [6] Hoover A. and Goldbaum M., "Locating the Optic Nerve in a Retinal Image using the Fuzzy Convergence of the Blood Vessels," *IEEE Transactions on Medical Imaging*, vol. 22, no. 8, pp. 951-958, 2003.
- [7] Hoover A., Goldbaum M., and Kouznetsova V., "Locating Blood Vessels in Retinal Images by Piecewise Threshold Probing of a Matched Filter Response," *IEEE Transaction on Medical Imaging*, vol. 19, no. 3, pp. 203-210, 2000.
- [8] Kabir H., Al-Wadud A., and Chae O., "Brightness Preserving Image Contrast Enhancement using Weighted Mixture of Global and Local Transformation Functions," *the International Arab Journal of Information Technology*, vol. 7, no. 4, pp. 403-410, 2010.
- [9] Lam B., Gao Y., and Liew A., "General Retinal Vessel Segmentation using Regularization-Based Multiconcavity Modeling," *IEEE Transactions on Medical Imaging*, vol. 29, no. 7, pp. 1369-81, 2010.
- [10] Lee S., McCarty C., and Taylor H., "Costs of Mobile Screening for Diabetic Retinopathy: A Practical Framework for Rural Populations," *Australian Journal of Rural Health*, vol. 9, no. 4, pp. 186-192, 2001.
- [11] Niemeijer M., "Comparative Study of Retinal Vessel Segmentation Methods on a New Publicly Available Database," in *Proceedings of International Society for Optical Engineering in Medical Imaging*, Florida, USA, pp. 648-656, 2004.
- [12] Niki N., Kawata Y., Satoh H., and Kumazaki T., "3D Imaging of Blood Vessels using Xray Rotational Angiographic System," in *Proceedings of International Conference Nuclear Science Symposium and Medical Imaging*, California, USA, pp. 1873-1877, 1993.
- [13] Rossant F., Badellino M., Chavillon A., Bloch I. and Pâques M., "A Morphological Approach for Vessel Segmentation in Eye Fundus Images with Quantitative Evaluation," *the Journal of Medical Imaging and Health Informatics*, vol. 1, no. 1, pp. 42-49, 2011.
- [14] Soares J., Leandro J., Cesar R., Jelinek F., and Cree M., "Retinal Vessel Segmentation using the 2-D Gabor Wavelet and Supervised Classification," *IEEE Transactions on Medical Imaging*, vol. 25, no. 9, pp. 1214-1222, 2006.
- [15] Sofka M. and Stewart C., "Retinal Vessel Centerline Extraction using Multiscale Matched Filters Confidence and Edge Measures," *IEEE Transactions on Medical Imaging*, vol. 25, no. 12, pp. 1531-46, 2006.
- [16] Staal J., Abramoff M., Niemeijer M., Viergever M., and Ginneken B., "Ridge Based Vessel Segmentation in Color Images of the Retina," *IEEE Transactions on Medical Imaging*, vol. 23, no. 4, pp. 501-509, 2004.
- [17] Vermeer K., Vos F., Lemij H., and Vossepel M., "A Model Based Method for Retinal Blood Vessel Detection," *Computers in Biology and Medicine*, vol. 34, no. 3, pp. 209-219, 2004.
- [18] Walter T. and Klein J., "Segmentation of Color Fundus Images of the Human Retina: Detection of the Optic Disc and the Vascular Tree using Morphological Techniques," in *Proceedings of the 2nd International Symposium on Medical Data Analysis*, London, UK, pp. 282-287, 2001.
- [19] Xiao Y., Cao Z., and Zhang T., "Entropic Thresholding Based on Gray-level Spatial Correlation Histogram," in *Proceedings of the 19th International Conference on Pattern Recognition*, Florida, USA, pp. 1-4, 2008.
- [20] Zhang B., Zhang L., and Karray F., "Retinal Vessel Extraction by Matched Filter with First-Order Derivative of Gaussian," *Computers in Biology and Medicine*, vol. 40, no. 4, pp. 438-45, 2010.



Soumia Belhadi is assistant professor at the University of Blida, she received the engineer diploma in electronic and her MS in image and sound processing from Blida University. Currently, she is member of the Image and Signal Processing Laboratory at the University of Blida. Her current research interests include: Medical image processing, computer vision, diagnostic aid.



Nadja Benblidia is senior lecturer at the University of Blida since 1984, she received the engineer diploma in computer science from University of Science and Technology Houari Boumediene (USTHB) and her PhD degree in electrical engineering and image processing from Blida University. In 2007, she obtained the PhD degree in space sciences at the University of Val de Marne (Paris XII). Currently, she is the director of the Research Laboratory for the Development of Computerized Systems at the University of Blida. She is a member of several scientific committees at the national and international level. Her current research interests include: Image processing, computer vision, information retrieval, data mining and pattern recognition in various fields especially medical, satellite, security.